Nanoscale subsurface plasma dynamics observed by single pulse GISAXS

When an intense femtosecond laser pulse far above the material damage threshold is irradiated on a solid, the atoms are immediately ionized, and a dense plasma is created. The laser field interacts with electrons around the surface up to tens of nanometers limited by the skin depth. After the laser pulse, several physical processes occur inside the material leading to thermalization, diffusion, compression, and ablation and finally resulting in a new surface structure [1]. A deeper understanding of these processes will enable better control of high-precision material processing and functional surfaces production.

Up to now, we are missing methods for observing these complex density dynamics with sufficient spatial and temporal resolution which prevented us from obtaining a quantitative understanding of the underlying physics. Here, we demonstrated for the first time the feasibility of single pulse grazing-incidence X-ray diffuse scattering experiments from laser-excited solids employing single XFEL pulses.

The experiment was performed at SACLA **BL2** EH6. A metallic multilayer (ML) sample consisting of five layers of tantalum (Ta) and copper nitride (Cu_3N) was irradiated by an optical laser with 800 nm wavelength, 3.6×10^{14} W/cm^2 intensity and 40 fs pulse duration (Fig.1(a)) [1]. After a variable delay, the sample was irradiated with 8.81 keV X-rays at a grazing-incidence angle of 0.64° and the scattered X-ray photons around the specular reflection were recorded by an MPCCD area detector [2]. To cover the X-ray footprint on sample (4 μm for 0.64° grazing incidence yields 360 μm), the laser beam was defocused to a diameter of ~500 μm. The intense specular reflection was blocked by a beam stop.

Figure1(b) shows the time evolution of the signal within the scattering plane at $Q_y = 0$ for time delays up to 4.0 ps. The intense peak at $Q_z = 1.33$ nm^{-1} represents the typical length scales of each Ta/Cu_3N double layer. The Kiessig fringes, represented as small peaks between $Q_z = 1.0$ and 1.33 nm^{-1}, are a fingerprint of the number of double-layer repeats in the ML sample [3].

Upon interactions with the laser, we observe drastic changes in the X-ray scattering profiles. We notice a progressive reduction of the number of Kiessig fringes with time and simultaneously, a broadening and reduction in intensity of the peak at 1.33 nm^{-1} both indicating a receding surface and a loss of correlation within the double-layer structure. The scattering signal at exit angles below the incident angle ($Q_z < Q_{specular}$) in the range of the critical angles of total external reflection (so-called Yoneda peaks) are originating predominantly from the interference of the topmost surface layers and are a sensitive marker for the structure of the uppermost layers. Even at the delay time of 4 ps, where the Kiessig fringes had disappeared, the Yoneda peaks are still present thus revealing important information for the density reconstruction.

We reconstructed the density profiles of the scattering signals using the state-of-the-art GISAXS analysis program BornAgain. Circular dots in Figs. 2(a) and 2(b) show the in-plane scattering signal obtained at –0.5 and 2.0 ps after the laser intensity peak. The solid lines in Figs. 2(a) and 2(b) represent refinements of the scattering data leading to the corresponding electron density profile shown in Fig. 2(c). While the density profile at –0.5 ps is identical to that of the cold sample, at 2.0 ps delay the density profile is strongly modulated although the periodic double-layer structure is still existing. A reduced number of layers or reduced homogeneity in layer thickness corresponds to the disappearance of Kiessig fringes between $Q_z = 1.0$ and 1.33 nm^{-1}. Furthermore, the reduced density of the uppermost Ta layer in Fig. 2(c) is corroborated by the reduction of the $Q_z = 0.87$ nm^{-1} peak.

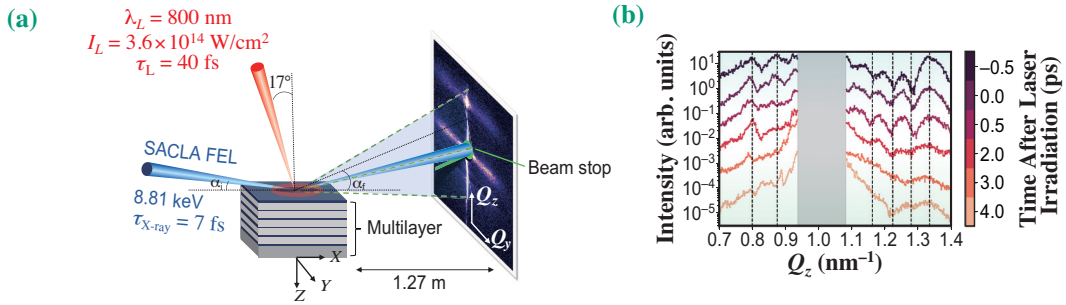

Fig. 1. **(a)** Experimental setup at SACLA BL2 EH6. **(b)** In-plane scattering signal for different time delays between laser and XFEL.

The reconstructed density profiles for different delays have been compared to two simulation codes: MULTI-fs, designed for femtosecond laser-solid interactions in a nonrelativistic regime [4] and PICLS, typically used for the modeling of relativistic plasmas in the context of, e.g., laser particle acceleration [5].

For both, simulations and experiment we observe an immediate expansion of the top layer into the vacuum due to high surface pressures (Fig. 3). Subsequently, the electron heat wave propagates into the bulk to heat the ML above 10 eV (~10^5 K) which modulates the ML structures. The observed ML dynamics in MULTI-fs appeared very different from our experiment which we attributed to the intermixing of particles between layers that is missing in the Lagrangian code. On the contrary, although kinetic PIC simulations have been considered inadequate for a relatively low temperature and highly collisional plasmas, the overall shape of the density profiles and the number of density peaks shows good qualitative agreements. This was achieved by implementing atomic-scale collisions into our PIC code. The agreement is however lost after ~2 ps due to the current limitations of the code: missing physics of radiation transport, multidimensional atomic mixing, recombination, large-angle many-body collisions, and degeneracy. This will motivate the development of new models which can now be tested by using our experimental method.

In summary, we demonstrated for the first time a new experimental capability of studying nanoscale surface and sub-surface dynamics upon high-intensity laser irradiation by grazing-incidence X-ray scattering with picosecond time resolution. Our result will allow the benchmarking of physics models and simulations with relevance to laser material processing and high-energy-density science.

For future experiments, having a larger detection area would be beneficial to provide additional constraints on the density retrieval. Additionally, a nanofocused X-ray beam would yield better time resolution to also observe femtosecond density dynamics.

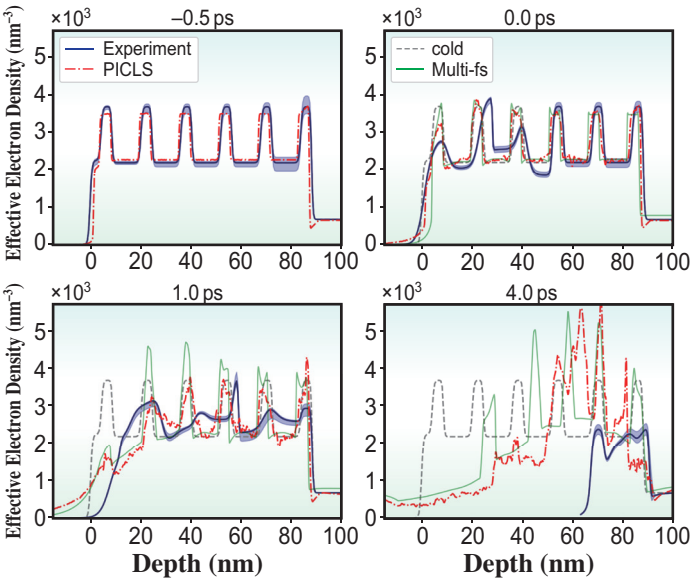

Fig. 3. Evolution of the electron density profiles with various pump-probe delays. Comparison between the experiment and simulations. Blue solid lines display experimental results, red dashed-dotted lines are simulation results from PICLS, and green solid lines are results from MULTI-fs.

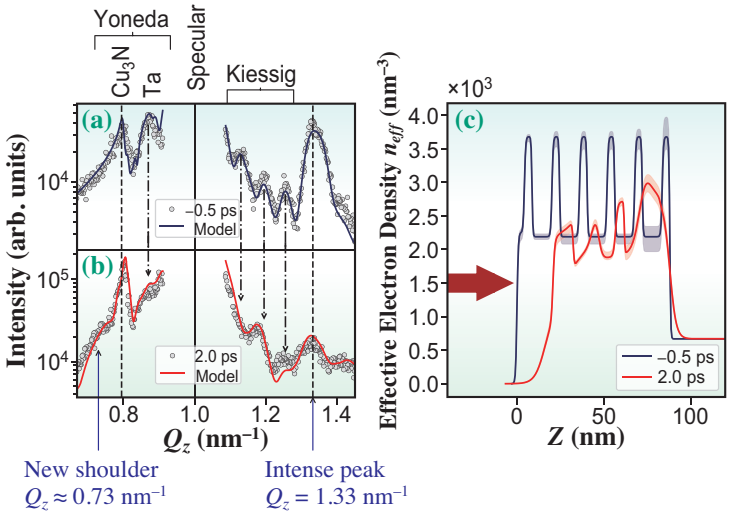

Fig. 2. GISAXS signals and corresponding electron density profiles. Lineout of the in-plane scattering at **(a)** 0.5 ps before and **(b)** 2 ps after the laser. **(c)** Retrieved electron density profile as a function of the depth.

L. Randolph[a,b,*], M. Banjafar[b], C. Gutt[a] and M. Nakatsutsumi[b]

[a] University of Siegen, Germany
[b] European XFEL, Germany

*Email: lisa.randolph@xfel.eu

References

[1] *L. Randolph, M. Banjafar, T. R. Preston, T. Yabuuchi, M. Makita, N. P. Dover, C. Rödel, S. Göde, Y. Inubushi, G. Jakob, J. Kaa, A. Kon, J. K. Koga, D. Ksenzov, T. Matsuoka, M. Nishiuchi, M. Paulus, F. Schon, K. Sueda, Y. Sentoku, T. Togashi, M. Bussmann, T. E. Cowan, M. Kläui, C. Fortmann-Grote, L. Huang, A. P. Mancuso, T. Kluge, C. Gutt and M. Nakatsutsumi: Phys. Rev. Res.* ***4*** *(2022) 033038.*
[2] T. Kameshima *et al.*: Rev. Sci. Instrum. **85** (2014) 033110.
[3] V. Holý *et al.*: Phys. Rev. B **47** (1993) 15896.
[4] R. Ramis *et al.*: J. Comput. Phys. **227** (2008) 6846.
[5] Y. Sentoku and A. J. Kemp: J. Comput. Phys. **227** (2008) 6846.